

Design and parametric analysis of composite transmission shaft for unmanned aerial vehicle (UAV)

Lai Zhang[#], Ze Qiao[#], Yisu Tao[#], Yiqiang Mu^{*}

Shenyang Aerospace University Shenyang, China

^{*} Corresponding Author Email: myq@sau.edu.cn

[#]These authors contributed equally.

Abstract. The lightweight design of aircraft is essential in improving efficiency, increasing flexibility, and improving aircraft safety. This article takes the lightweight design of unmanned aerial vehicles as a research question. Different single-layer thicknesses and four laying sequences have been designed for lightweight transmission shafts. Through simulation analysis of various arrangements on the transmission shaft, we know that the 45 ° ply angle can increase the torsional performance of the shaft by 50% r reduce natural frequency by 25%, and when only considering the torsional strength of the shaft body, it is a better ply scheme to increase the ply order by 45° between 0° and 90°. The proposed design connection structure and the selected arrangements can reduce the weight of the drive shaft and complete the UAV lightweight goal.

Keywords: Composite transmission shaft, UAV, finite element analysis, parametric analysis, ANSYS.

1. Introduction

Recently, composite materials have been widely used to reduce weight [1]. Modern aircraft structure requires higher specific strength and specific stiffness, and composite materials meet this requirement. The amount of high-performance composite materials, especially carbon fiber-reinforced resin matrix composite materials, has become an important index to measure the advancement of civil machinery [2]. Compared with traditional metal materials, carbon fiber composites have the advantages of high specific strength, and strong design ability, which are widely used in national defense science and technology[3]. Due to the design ability of the composite, it is increasingly used in the manufacture of high-speed rotation and large aspect ratio drive shafts, the American RAH-66 Comanche drone [4]. Compared with the metal drive shaft, the carbon fiber composite drive shaft is light and has the advantages of high specific strength and good safety performance [5]. In designing and manufacturing UAV composite drive shafts, the kinetic characteristics are considered [6], and the mechanical system can easily produce resonance in the operation process[7]. The drive shaft made by carbon fiber composite material can significantly reduce the weight of the structure, but improve the natural frequency, effectively reduce the noise, reduce the energy loss of the transmission system, and enhance the anti-vibration performance.

The transmission shaft is a high-speed, less supporting rotating body, and the main role is power transmission. The transmission shaft is mainly for contact stress and fatigue crack expansion and material lightweight design. For example, Li et al. [8] completed the drive shaft contact stress and fatigue crack extension analysis of unmanned aerial vehicles, Soliman Ehab Samir Mohamed Mohamed[9]. The basic structural form of carbon fiber reinforced composite drive shaft is established by optimizing the sequence of composite drive shaft layers. The carbon fiber composite drive shaft was developed by Centa Company[10]. The maximum rated torque can reach 335 kNm, and the shaft length can reach 8 m to 10 m. The company has specially developed computer programs to design the most effective fiber bedding structure so that the propulsion shaft has good technical characteristics[11].

To reduce the weight of the transmission shaft while still avoiding failure, we need to understand the failure mechanism. Generally speaking, the causes of composite material failure mainly include fiber fracture, matrix crack, interface shear, and failure mode transfer[12]. Fiber breaking: the fibers

in composite materials are generally isotropic, and their tensile strength can reach a very high level. However, when the fiber is excessively bent, squeezed, or stretched, it leads to fiber breakage. According to the comparison of the allowable stress level and the tensile strength of the fiber, the fiber breaking can be divided into two conditions: pull and shear[13]. Matrix crack: the composite material matrix is generally anisotropic material with strong compressive strength. However, because it is less resilient than fibers, the matrix strength will be the main factor in the application of composite materials. When cracks or microcracks appear in the matrix, the strength of the whole material will decrease and even cause the collapse of the material[14]. However, due to specific properties of the fiber, such as the surface energy, the relaxation, etc., [15]. The shear failure generally occurs under high-stress or high-temperature conditions.

The paper uses ANSYS software to establish the geometric model of the finite element. After establishing the basic parameters of the drive shaft, apply the constraints and fixed torque of the transmission shaft of the driving shaft, and then the failure of the shaft is obtained through the Tsai-Wu failure criterion. The laying angle of 45° can improve the torsion resistance of the shaft body by 50%, and the natural vibration frequency is reduced by 25%. It is better to increase the laying order of 45° between 0° and 90° . To verify the feasibility of the optimization method, analyze the model on the selected finite element analysis model, check the strength of the material, and analyze the kinetic behavior and stability of the structure. At the same time, the paper studies and understands the connection structure design scheme of UAV composite drive shaft and proposes the feasibility basis for using carbon fiber as the drive shaft.

2. The fundamental design of composite transmission shaft

2.1. Theoretical and design basis of the composite transmission shaft

Usually, we think of fiber winding products as lamination plate structural parts, so the design criteria and design requirements of lamination plate products are also applicable to fiber winding products. Laminate design mainly includes laying order, paving angle, and determining the proportion of various paving angles [16]. Therefore, the principle of minimum proportion should be followed in the design of composite laminate[17]. To ensure that the angle of the fiber between the two layers is greater than or equal to 45 degrees to improve the strength of the lamination plate and simultaneously coordinate the Poisson ratio of the composite and the connected metal, and reduce the stress caused by the connection. To facilitate the finite element analysis, ring T700 is detailed in this section [18], and the finite element modeling of the drive shaft is established for the material. The carbon fiber hollow shaft is set at $\text{Ø} 46 * \text{Ø} 40 * 200$. The metal pin size is $\text{Ø} 6 * 20\text{mm}$. The geometric dimension of the composite transmission shaft is shown in Figure 1.

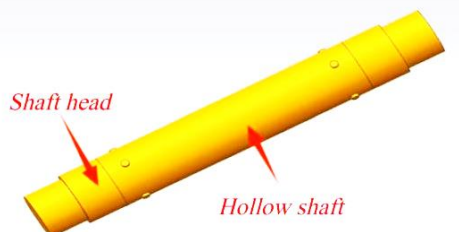


Figure 1. Image of composite transmission shaft for UAV

2.2. Tsai-Wu failure criterion

Tsai-Wu failure criteria[19] divide material failure into two conditions: tensile failure and compression failure. The composite structure is positive in the tensile failure case. In the compression failure case, the main stress is negative. The strength factors in the Tsai-Wu failure criterion include tensile strength, compressive strength, shear strength, torsional strength, and alternating strength, which are adjusted and optimized according to the actual situation of composite material. The Tsai-

Wu criterion is expressed in the form of a tensor. Tensors are mathematical tools representing matter properties and laws of change, which can describe physical quantities in multiple directions and conditions and serve as generalizing vectors and matrices. In the Tsai-Wu criterion, the coefficient matrix is also a tensor and is composed of multiple components, which reflects the strength properties and material properties of the composite in all directions. Therefore, adopting the tensor formalism allows for a more intuitive and accurate description of the strength properties of composites.

For the 2D plane stress state ($\sigma_3 = 0, \tau_{13} = 0, \tau_{23} = 0$), The Tsai-Wu failure criterion is expressed as follows:

$$F_1\sigma_1 + F_2\sigma_2 + 2F_{12}\sigma_1\sigma_2 + F_{11}\sigma_1^2 + F_{22}\sigma_2^2 + F_6\tau_{12} + F_{66}\tau_{12}^2 = 1 \quad (1)$$

Orthogonal anisotropic Tsai-Wu, the coefficient F_{ij} of the failure criterion related to the material strength parameters of the composite lamina, and it can be calculated by the formula:

$$F_1 = \left(\frac{1}{X_1^T} - \frac{1}{X_1^C}\right), F_2 = \left(\frac{1}{X_2^T} - \frac{1}{X_2^C}\right) \quad (2)$$

$$F_{12} = -\frac{1}{2} \sqrt{\frac{1}{X_1^T * X_1^C} * \frac{1}{X_2^T * X_2^C}}$$

$$F_{11} = \frac{1}{X_1^T X_1^C}, F_{22} = \frac{1}{X_2^T X_2^C} \quad (3)$$

$$F_6 = \left(\frac{1}{X_{12}^T} - \frac{1}{X_{12}^C}\right), F_{66} = \frac{1}{X_{12}^T * X_{12}^C}$$

Where X_1^T represents the tensile material strength of the thin layer along the fiber direction, X_1^C represents the compressive material strength of the thin layer along the fiber direction, X_2^T represents the tensile material strength of the thin layer in the transverse fiber direction, X_2^C represents the compressive material strength of the thin layer in the transverse fiber direction, X_{12}^T represents the positive shear strength of the thin layer, and X_{12}^C represents the negative shear strength of the thin layer.

The Tsai-Wu criterion is expressed as a tensor. Tensor [20] is a mathematical tool representing material properties and laws of change that can describe multiple directions and different forms of physical quantities and serve as a generalizing extension of vectors and matrices. In the Tsai-Wu criterion, the coefficient matrix is also a tensor and is composed of multiple components, reflecting the strength properties and material properties of the composite in all directions. Therefore, adopting the tensor formalism allows for a more intuitive and accurate description of the strength properties of composites. In contrast, other strength criteria are often only applicable to the coordinate system of the main axis direction of the material. Its coefficients do not have the formal representation of the tensor and therefore are not well applicable to other coordinate systems. It makes the Tsai-Wu criterion a great advantage in engineering applications. The stress state of the lamins calculated by the program can be expressed by using the following components: σ_1 , σ_2 and τ_{12} .

The Tsai-Wu failure criterion predicts material failure under uniaxial stretch, compression, shear, torsion, and alternating loads. The Tsai-Wu failure criterion is also widely used in engineering practice because of its perfect mathematical form and accurate calculation results. In particular, in aerospace, automotive, ships, and sports equipment, the Tsai-Wu failure criterion has become an essential tool for optimizing the design of materials and components to improve product performance and reliability.

3. Finite element modeling of the composite transmission shaft

3.1. Material property

The drive shaft connection structure mainly includes the metal shaft head, pin, and carbon fiber composite drive shaft. To facilitate the experiment and reduce the experimental cost, the inner holes of the metal shaft and the composite air core shaft are connected by a pin, and the pin and the hole on the metal shaft head and the composite air core shaft for zero clearance. According to the data, the torque size received by the intermediate shaft is $650\text{N} \cdot \text{m}$. Considering the hollow axis of carbon fiber, the mechanical property parameters of the T700 carbon fiber reinforced composite belt are shown in TABLE I. Metal shaft head structure steel material properties are shown in Table II.

Table 1. Carbon fiber T700 material properties [21]

Mechanical properties	CFRP data
density (g/cm^3)	1.8
X-direction elastic modulus (MPa)	1.15×10^3
Y-direction elastic modulus (MPa)	6430
Z-direction elastic modulus (MPa)	6430
The Poisson's ratio in the XY direction	0.28
The Poisson ratio of the YZ direction	0.34
The Poisson ratio of the XZ direction	0.28
XY direction shear modulus (MPa)	6000
YZ-direction shear modulus (MPa)	6000
XZ-direction shear modulus (MPa)	6000
Tensile strength in the X-direction (MPa)	1500
Y-direction tensile strength (MPa)	30
Z-directional Tensile Strength (MPa)	30
X-direction compression modulus (MPa)	700
Y-direction compression modulus (MPa)	100
Z-direction compression modulus (MPa)	100
XY direction shear modulus (MPa)	60
YZ-direction shear modulus (MPa)	30
XZ-direction shear modulus (MPa)	60

Table 2. Metal shaft head structure steel material properties[22]

Mechanical properties	Metal data
density (g/cm ³)	7.85
Elastic modulus (MPa)	200
Poisson ratio	0.3
Tensile Strength (MPa)	460
Yield Strength (MPa)	250

3.2. Composite layup angle arrangement

To determine the laying scheme of the composite pipe, it is necessary to understand the effect of the laying angle[23] on the connecting structure of the composite drive shaft. Some important factors are determined the torsion of the connection structure[24], such as deformation of the drive shaft, maximum shear stress of metal shaft head and sleeve, failure of carbon fiber composite pipe, and torsion angle of the drive shaft. The design requirements of the transmission shaft further improve the shaft performance. The comparative analysis results provide the basis for the orientation design [25]. According to scenario 1: [45/-45/90/45/-45]s, scenario 2: [90/0/-45/45/ 0]s, scenario 3: [90/-40/45/0 /45]s, scenario 4: [-45/45/45/-45/45]s go through the above finite element analysis process are presented in Figure 2.

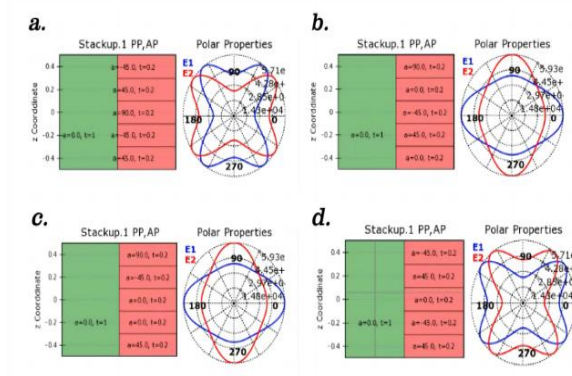


Figure 2. Four different angle laying schemes with a thickness of 0.2mm: (a): [45/-45/90/45/-45]s; (b): [90/0/-45/45/0]s; (c): [90/-45/0/0/45]s; (d): [-45/45/0/-45/45]s;

3.3. Boundary and loading conditions

If a structure has no boundary conditions[26], then the stiffness matrix of this structure is considered a singular matrix. Furthermore, a rigid structure moves if it has no constraints with 6 degrees of freedom or does not satisfy the required constraints. Therefore, when analyzing the deformation size and relative position of the structure, it is necessary to examine the boundary conditions to avoid the displacement phenomenon. Pins connect the carbon fiber composite pipe. Since only linear structure analysis is considered in this paper, Bound constraint is used between all components. In the process of UAV flight, the transmission shaft is mainly affected by the torsion force. According to the design requirements of the transmission shaft, it is known that the maximum torsional force of the transmission shaft is 650N · m. To simulate experimental conditions, torque is applied on one end of the drive shaft and fixed restraints on the other, as shown in Figure 3.

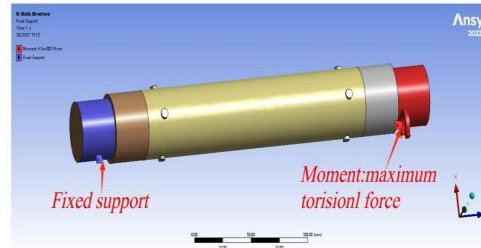


Figure 3. Loading and constraint conditions of the composite transmission shaft in the finite element modeling

4. Results and discussion

4.1. Results of the composite transmission shaft

Post-treatment yielded the carbon fiber hollow axis stress cloud map, as shown in Figure 4. The carbon fiber hollow axis is at least 303.29MPa at [45 / -45 / 90 / 45 / -45]s. It occurs in the direction of the torque shaft head connected to the inner wall of the shaft head. Figure 3 illustrates the total deformation of the carbon fiber transmission shaft under four laying schemes, and the failure index comparison results of carbon fiber composite materials were obtained[27] according to the failure state predicted according to the Tsai-Wu criterion, as shown in Figure 4.

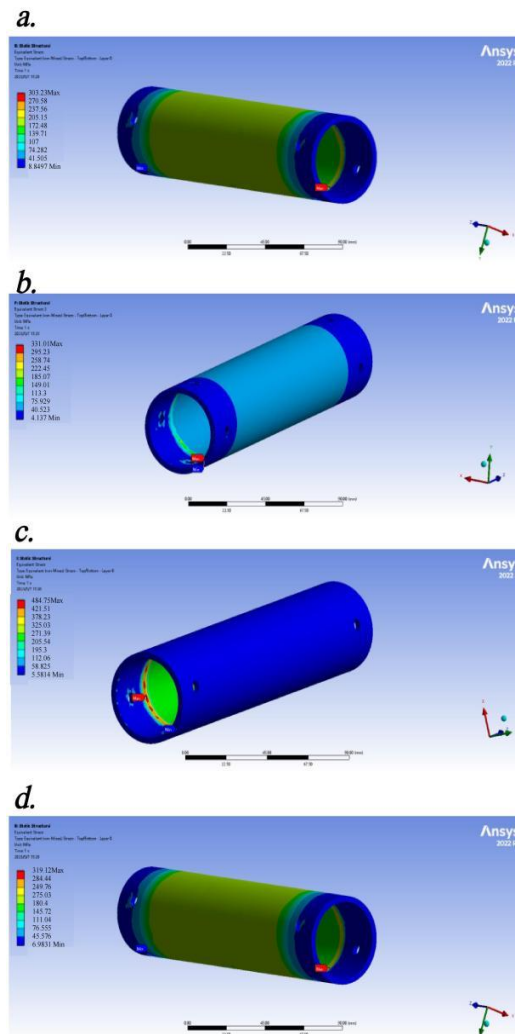


Figure 4. Nominal stress of carbon fiber of different layered schemes with a thickness of 0.2 mm:
 (a) Scheme for [45/-45/90/45/-45]s; (b) Scheme for [90/0/-45/45/0]s; (c) Scheme for [90/-45/0/0/45]s; (d) Scheme for [-45/45/0/-45/45]s

The total deformation of the carbon fiber transmission shaft under four layering schemes is: Scheme 1 is 0.54226mm. Option 2 is 0.84102 mm. Option 3 is 0.83772mm. Option 4 is 0.54425mm, and the failure index result of carbon fiber composite material is: Option 1 is 0.75. Option 2 is 1.125. Option 3 is 1.125. Option 4 is 1.125. As shown in the above dates, the drive shaft of schemes 2 and 3 is greatly deformed, and the failure of carbon fiber material is the most likely. Compared with Scheme 1 and 4, the drive shaft deformation of Scheme 1 and 4 is smaller. Because 0° is stronger than 90° , the carbon fiber composite tube of Scheme 4 is more likely to fail. After the finite element analysis process, the stress cloud map of the carbon fiber shaft head is shown in Figure 5. Axle head at $[45 / -45 / 0 / 45 / -45]_s$. The minimum force in the laying order is 798.02MPa. It occurs in the direction of the torque shaft head connected to the inner wall of the shaft head[28].

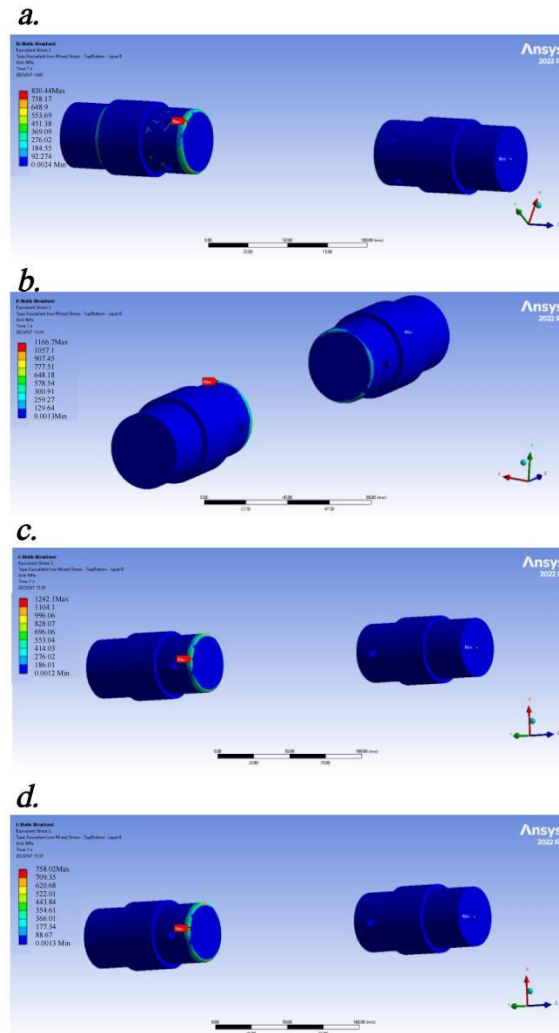


Figure 5. Stress cloud chart of shaft head with a thickness of 0.2mm for different laying schemes:a.Scheme for $[45/-45/90/45/-45]_s$ b.Scheme for $[90/0/-45/45/0]_s$ c.Scheme for $[90/-45/0/0/45]_s$ d.Scheme for $[-45/45/0/-45/45]_s$

After the finite element analysis, the post-processing obtained the carbon fiber axis population, and the stress cloud map is shown in Figure 6. The overall deformation at $[45/-45/90/ 45/-45]_s$. The minimum deformation of the laying order[29] is 0.54226mm. It occurs in the top area in the direction of the torque shaft.

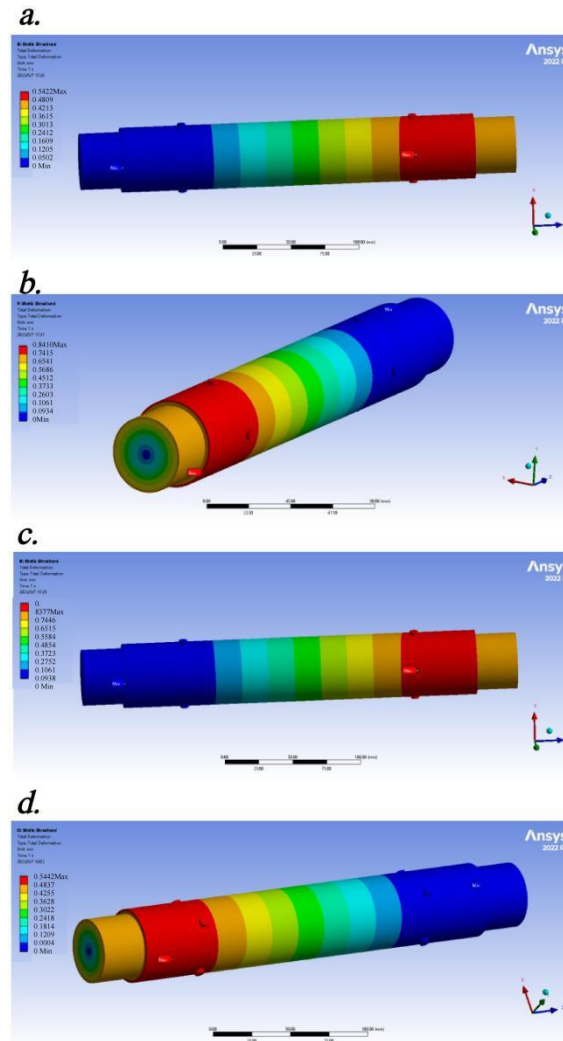


Figure 6. Stress cloud chart of shaft head with a thickness of 0.2mm for different laying schemes:a.Scheme for [45/-45/90/45/-45]s b.Scheme for [90/0/-45/45/0]s c.Scheme for [90/-45/0/0/45]s d.Scheme for [-45/45/0/-45/45]s

For the metal shaft head, the stress of the four laying schemes is small, scheme 2 and 3 is large, and the stress of scheme 4 is minimum. In the case of choosing scheme 1, the metal shaft head is less easy to destroy in the action of the torsion force, so the connection structure is less easy to fail. In conclusion, the final paving scheme is selected as Scheme 1.

4.2. Effect of the wall thickness

Under protocol [45 / -45 / 90 / 45 / -45]s. The single-layer thickness[30] was 0.2mm and 0.1mm, respectively. After the finite element analysis, the carbon fiber hollow shaft and metal shaft head stress cloud map were obtained and shown in Figure 7.

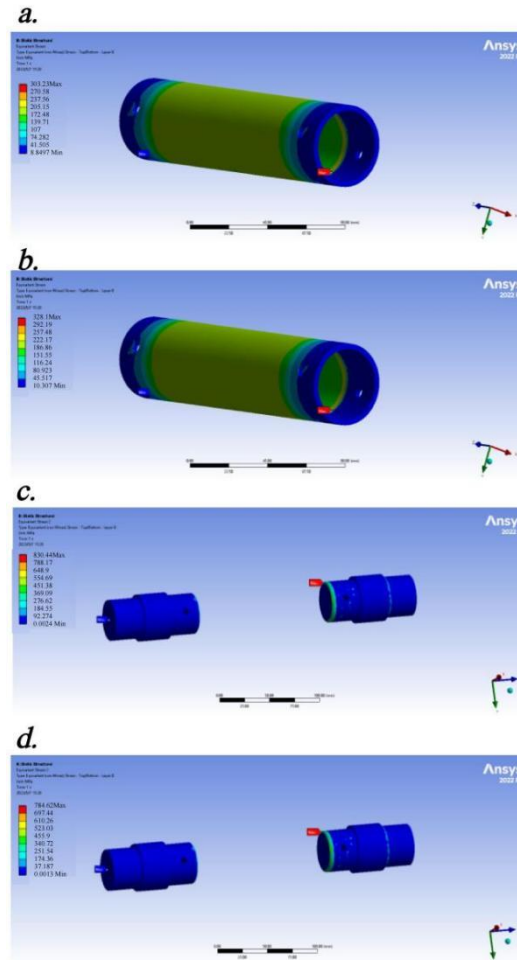


Figure 7. Stress cloud chart of carbon fiber hollow shafts with different thicknesses under the [45/-45/90/45/-45] s scheme:a.Scheme for [45/-45/90/45/-45]s b.Scheme for [90/0/-45/45/0]s c.Scheme for [90/-45/0/0/45]s d.Scheme for [-45/45/0/-45/45]s

The carbon fiber hollow shaft is covered at 0.2mm single layer thickness[31] so that the minimum stress is 303.29MPa, which occurs in the direction of the inner wall of the shaft head. The shaft head at 0.1 single layer thickness makes the stress of 784.62MPa, which occurs in the direction of the torque shaft head connected to the inner wall of the shaft head.

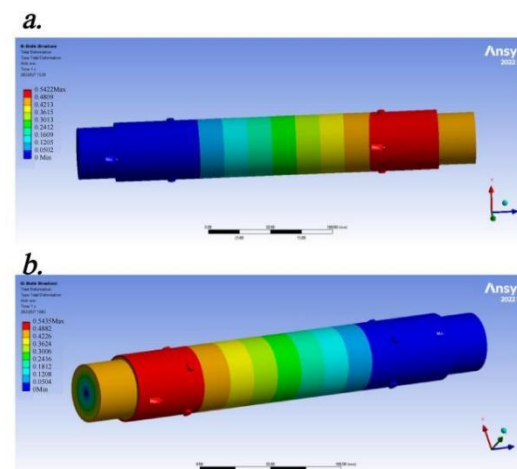


Figure 8. Overall stress cloud charts of different thicknesses under the [45/-45/90/45/-45] s scheme:a.Thickness 0.2mm b.Thickness 0.1mm

Figure.8 presents the minimum deformation, which is 0.54226mm at the thickness of 0.2, which occurs in the top area in the direction of the torque shaft. Figure. 10 presents per protocol [45 / -45 /

90 / 45 / -45]s. The carbon fiber hollow shaft is laid in 0.2mm single layer thickness to make the minimum stress of 303.29MPa, which can meet the torque of 650N / m. The thickness of the shaft head in 0.1 single layer makes the stress of 784.62MPa. In this condition, the force is greater than the yield strength of structural steel of 250MP a, or even higher than its maximum tensile strength of 460MP a, so the shaft head must fail[32].

4.3. Effect of composite layup angle on the nature

During the flight of the UAV, the rotor may vibrate due to the action of airflow[33]. The rotor works through the power transmitted by the bevel gears. Since the inner drive shaft of the arm needs to be connected to the local gear in the gearbox, the inner shaft of the arm is more likely to vibrate compared with the middle shaft. Then, this section will explore the influence of the laying mode on the natural frequency of the inner shaft of the arm. Mechanical vibration theory can explain the related phenomena in life and the theoretical knowledge that must be referred to when designing mechanical products[34].

Therefore, it is of great significance to study the influence of different laying modes on the natural frequency of the connection structure to ensure the stability of the transmission shaft. Through the ANSYS finite element software. The vibration of the carbon fiber tube can be represented as a linear combination of natural frequencies[35], in which the low-order vibration pattern plays a decisive role in its dynamic properties. After fixing one end of the drive shaft and applying torque, the degree of freedom at the other end is analyzed. Since the influence of the paving scheme on the performance of the connection structure has been analyzed above, the natural frequency of the drive shaft will also impact the performance of the connection structure. Therefore, it adds mode analysis, imposes zero displacement constraint on the side of a drive shaft, and loads the mode of the first four orders[36] to conduct analysis.

The analysis results are shown in Figure 9. There is no obvious difference between the natural frequency of order 1 and order 2 of the four schemes, while the natural frequency of order 1 is reduced by 25% from order 3 to order 4. The comparison of the natural frequency of the drive shaft under different laying sequences is shown in Figure 11. The laying order does not significantly affect the vibration shape, but the bending vibration amplitude of order 1 and order 2 is small. However, the bending vibration occurs from the order 3 to order 4. The natural frequency can be effectively increased by improving the bending stiffness of the drive shaft.

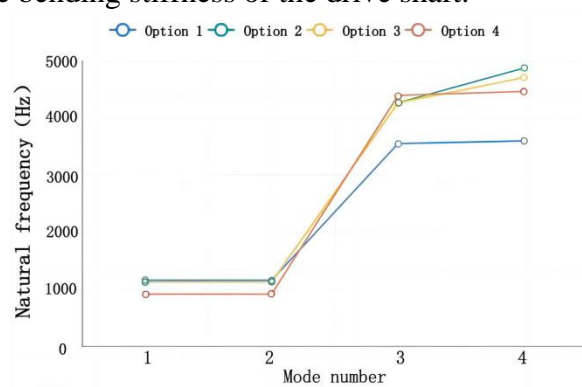


Figure 9. The relationship between laying sequence and natural frequency

As shown in Figure 9, in contrast, a single layer of 0.2mm thick carbon fiber strip was used [45/-45/90/45/-45]s. As the laying scheme of carbon fiber composite transmission shaft, the laying scheme can reduce the probability of resonance phenomenon and thus make the operation of the UAV more stable, prolonging the transmission shaft and the UAV service life and reducing the noise[37]. It can be seen that the natural frequency increases monotonically with the decrease of the laying angle. Therefore, when designing the carbon fiber composite drive shaft, the number of small angles can be appropriately increased to increase the natural frequency of the drive shaft to stay away from the critical speed when working.

5. Conclusion

This paper uses ANSYS analysis software to design four different paving schemes by modeling and finite element analysis. The appropriate laying scheme should be selected according to the specific application scenario to ensure that the drive shaft has sufficient strength and stiffness under normal working conditions and that no failure or failure will occur. The following conclusions are drawn: The 45° laying angle can improve the torsion resistance of the connecting structure by 50%, and the 45° laying angle in the innermost and outermost layer of the composite material is conducive to improving the torsional performance of the connecting structure. It is adopted a single layer of 0.2mm thick carbon fiber directional belt to [45 / -45 / 90 / 45 / -45]s. The strength and stiffness of the carbon fiber hollow shaft in the laying scheme are better than the other four. While the vibration amplitude at order 3 to 4 is 25% lower than the other schemes. By improving the bending stiffness of the drive shaft, its natural frequency can effectively prevent vibration.

References

- [1] Shen Haojie; Xia Yang; Chen Gang, Topology optimization design of embedded skeleton of a certain UAV wing. *Computer Simulation*, 2022.
- [2] Luo Yunfeng, Yao Jiana., Application of high-performance thermoplastic composites in the civil aviation field. *Aviation Manufacturing Technology*, 2021.
- [3] Zhang Yin, Innovation reform and practice of teaching mode, *Modern Vocational Education*, 2020.
- [4] Fan Huibing, Guo Jinlong, Luo Guangwen, The application of drones in modern warfare, light weapons, 2022.
- [5] CAI Guangsheng, Zhang Jinguang, MAO Ge, Design of carbon fiber composite, *FRP Composites*, 2019.
- [6] Progress in the study of dynamic modeling of no human-computer interaction operation, *Aviation Journal* 2022.
- [7] Y, L., Zhao, D, X., Cao, J, E., Chen Nonlinear dynamics of a Z-shaped structure with validated global analytical mode shapes, *Communications in Nonlinear Science and Numerical Simulation*, 2020.
- [8] Li Long, Yu Tianxiang, Shang Bolin, Song Bifeng, Chen Yijia, Analysis of Contact Stress and Fatigue Crack Growth of Transmission Shaft, *Journal of Failure Analysis and Prevention*, 2023.
- [9] Darrow; Donald C, COMPOSITE SHAFT WITH INTEGRAL END FLANGE, United States Patent: 3651661, Mar, 28, 2022.
- [10] Zeyu Sun, Jie Xiao, Xuduo Yu, Rogers Tusiime, Hongping Gao, Wei Min, Lei Tao, Liangliang Qi, Hui Zhang, Muhuo Yu Vibration characteristics of carbon-fiber reinforced composite drive shafts fabricated using filament winding technology *Journal Composite Structures*, 2020.
- [11] Samuel Mosopefoluwa, Tayong Rostand B, 3D numerical analysis of the structural behaviour of a carbon fibre reinforced polymer drive shaft, *Journal Results in Engineering*, 2023.
- [12] Wang Han, Yang Yuzhu, Analysis of the tensile failure mechanism of carbon fiber composite laminates based on finite element simulation, *Journal of Textile Science and Engineering*, 2023.
- [13] Lv Qingquan, Zhao Zhenqiang, Li Chao, Zhang Chao, 2.5D Progressive damage and failure simulation of woven composite materials, *Journal of Composite Materials*, 2021.
- [14] Chen Li; Jiao We, Wang Xinmiao, Liu Junling, Progress on mechanical properties of 3 D woven composites, *Materials Engineering*, 2020.
- [15] Dang Xiaoyan, Ji Fei, Zhang Lei, Yang Weiping, Comparative analysis of different failure modes during high-speed impact of thermoplastic composites, *Equipment and Environmental Engineering* 2022.
- [16] Li Hui, Zhao Chunjiang, Liang Jianguo, Zeng Guang, Wang Rui, Bian Qiang, Analysis of mechanical characteristics and failure mechanism of variable stiffness composite laminate, *Composite Materials Science and Engineering*, 2022.
- [17] Shao Shuai Cao Hang Wang Xiangping Guo Yong Xu Hongming, Strength analysis and layer optimization design of aero-engine composite fan blade, *Gas Turbine Test and Research*, 2022.

- [18] Bai Heshan, Bai Ruixiang, Zhao Tianyu, Lei Zhenkun, Hong Xiang, Liu Chen, Wang Tao, Characterization of interfacial bonding properties of Vitrimer resin/ T700 fibre, *Composite Interfaces*, 2023.
- [19] Deng Songwen, Sheng Ying, Jia Bin, Wang Ruheng, Forecasting and test verification of composite material cylinder burst pressure based on Tsai-Wu failure criterion, *Journal of Southwest University of Science and Technology*, 2022.
- [20] Li Li, Bai Rui, Lu Jianfeng, Zhang Shanqing, Chang ChingChun A Watermarking Scheme for Color Image Using Quaternion Discrete Fourier Transform and Tensor Decomposition, *Applied Sciences*, 2021.
- [21] Wu Bo, Yang Changling, Zhang Linping, Lv Yonggen, *Progress in Composites Science and Engineering of Composites*, 2021.
- [22] O Krol, V Sokolov, P Tsankov, Modeling of vertical spindle head for machining center *Journal of Physics Conference Series*, 2020.
- [23] Quanjin Ma, M.R.M.Rejab, Mohammad, Azeemc, M.S.Idrisa, M.F.Ranid, A.PraveenKumar, Axial and radial crushing behaviour of thin-walled carbon fiber-reinforced polymer tubes fabricated by the real-time winding angle measurement system, *Forces in Mechanics*, 2023.
- [24] Liu Peng, Zheng Wan, Shen Shaofeng, Ming Jiangyong, Liang Zhenjiang, Wang Shuang, Zhang Huirong, SCR7000 Key influencing factors of torsion crack of continuous casting and rolling copper rod, non-ferrous metal engineering, 2023.
- [25] Ji Miaomiao, Zhang Housheng, Wu Qin, Zhang Hanzhe, Huang Biao, Wang Guoyu, Ply angle effects on cavitating flow induced structural response characteristics of the composite hydrofoils, *Ocean Engineering*, 2023.
- [26] Xiong Jiayuan, Han Duanjun, Tang Xiangjing, Tang Guangming, Study on pavement temperature field and influencing factors under periodic boundary conditions, *Value Engineering*, 2023.
- [27] Saif Tamara, Saad Najim, AlZubiedy Ali, Idzikowski Adam, Effect of ply angle on the burst pressure of composite pressure vessels by filament winding, *Construction of Optimized Energy Potential Budownictwo o Zoptymalizowanym Potencjale Energetycznym*, 2022.
- [28] Lee Hyoungwook, Kim ChulSu, Prediction of Ply Angles of Air Springs According to Airbag Positions and Their Effects on Lateral and Torsional Stiffness, *Applied Sciences*, 2022.
- [29] Yu Su, Yang Yunpei, Colton Jonathan S, Improved composite open-hole compression strength and trade-off with manufacturability controlled by stacking sequence effect and non-standard ply angles, 2022.
- [30] Li Xinyue, Yuan Yanan, Zhang Zuoqi, Gradient ply thickness design for enhanced low-velocity impact resistance in ultra-thin ply composite, *Extreme Mechanics Letters*, 2023.
- [31] Velasco M.L., Correa E., Sánchez-Carmona S., París F., Evolution of the damage onset and morphology in [0/90_n/0] laminates when increasing the ply thickness, *Composites Part A*, 2023.
- [32] Fanuc Corporation, Patent Issued for Failure Detection Device For Spindle Head Of Machine Tool Including A Plurality Of Sensors, *Journal of Robotics & Machine Learning*, 2019.
- [33] Pan Fei, Guo Shikang, Wang Zhijia, Li Shengmin, Study on the dynamic displacement test method of vibration table model based on UAV and optical flow characteristic value method, *Seismic Engineering and Engineering vibrations*, 2023.
- [34] Wang Yuan, exploration of basic course of mechanical vibration under the background of new engineering, *Modern Vocational Education*, 2019.
- [35] Zhao Fei, Wu Jinwu, and Zhao Longsheng, The hierarchical theory was used to calculate the natural frequency and vibration patterns of the lamina, *noise and vibration control* 2021.
- [36] Németh Róbert K, Geleji Borbála B, Modal truncation damping in reduced modal analysis of piecewise linear continuum structures, *Mechanics Based Design of Structures and Machines*, 2023.
- [37] Wei Kai, Cao Qi, Yan Qun, Xu Jian, Xue Dongwen, the UAV propeller aerodynamic noise test in the ground acoustic environment, *Science, Technology and Engineering*, 2023.